🔓**Open Access**

Simple and Flexible All-Optical Microwave Photonic Frequency Converter Based on Stimulated Brillouin Scattering Effect

Yue Wang
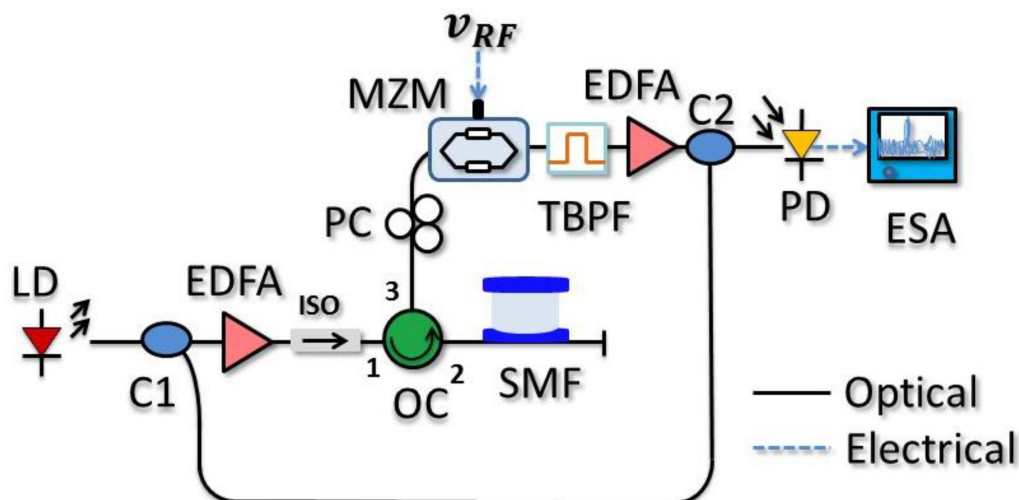**Weinan Zhou**
Yujiao Ding
Tongtong Meng
Wei Dong
Xindong Zhang

Simple and Flexible All-Optical Microwave Photonic Frequency Converter Based on Stimulated Brillouin Scattering Effect

Yue Wang [iD]**, Weinan Zhou, Yujiao Ding, Tongtong Meng, Wei Dong** [iD]**, and Xindong Zhang**

State Key Laboratory on Integrated Optoelectronics, College of Electronic Science and Engineering, Jilin University, Changchun 130012, China

Abstract: We present a novel and simple scheme for all-optical microwave photonic frequency converter, free of electrical components, based on stimulated Brillouin scattering (SBS) effect. An SBS-based frequency shifter is incorporated to generate Stokes wave whose frequency is down-shifted by v_b, where v_b is defined as the Brillouin frequency shift. With a tunable optical passband filter, the up/down frequency conversion can be realized through the same structure. In the proof-of-concept experiment, the microwave signal at 1 to 15 GHz can be up-converted while the microwave signal at 11 to 29 GHz can be down-converted by the microwave photonic frequency converter. Moreover, the frequency and power stability of the generated signals are also investigated in three hours. To vindicate flexibility, low cost and easy implementation of the proposed all-optical setup, an experiment is carried out, and it turns out that only the frequency-to-be-converted signal source is needed while providing the ultra-wideband up/down conversion.

Index Terms: Microwave photonics, frequency converter, stimulated Brillouin scattering, radio over fiber.

1. Introduction

Microwave photonic converter schemes are considered as promising applications in radar [1], wireless communication systems [2], modern electronic warfare receivers [3] and defense systems, owing to its inherent properties of ultrafast scanning, accurate beamforming and immunity to electromagnetic interference [4]. In recent years, with the requirement of high selectivity, high sensitivity, high frequency wide dynamic range, and wideband wireless receivers, millimeter-wave up/down-conversion system is developing rapidly. Optical components have low transmission loss and are lightweight, which make photonic microwave mixers more attractive for applications in harsh environments such as avionics, radar receivers, satellite payloads. To form a microwave converter, several methods have been put forward based on the frequency up/down conversion technique. Usually, a conventional microwave converter is used to convert high-frequency radio

frequency (RF) signal to intermediate frequency (IF) signal [5], [6]. The challenges of the conventional microwave converter include the limited bandwidth and low channel isolation. Generally, frequency conversion is an effect caused by the nonlinearity [7]. Photonic frequency conversion has been studied in different literatures based on the different nonlinear media. For instance, semiconductor lasers can be used for photonic frequency conversion. On account of the strong nonlinear effects, such as four-wave mixing, cross-gain modulation, cross-polarization modulation and cross-phase modulation [8]–[11], the semiconductor optical amplifier (SOA) is also a promising device for realizing photonic frequency conversion. The main problem of SOA-based techniques is the poor signal quality after conversion. To overcome these challenges, various methods have been intensively investigated, which is convenient to implement, such as using two cascaded Mach–Zehnder modulators (MZMs) [12], a pair of phase modulators (PMs) interrelate in series [4], and a dual-polarization dual-parallel Mach-Zehnder modulator (DP-DPMZM) technology [13] to up/down-convert the signal. However, the two modulators and DPMZM utilized in the above techniques result in the power attenuation caused by the loss of the devices, which will degrade the performance of the long-haul transmission. The desirable IF signal generated at photodetector (PD) is disturbed by lots of mixing spurs because of the MZMs are cascaded [12]. In order to suppress the mixed spurs generated between optical carriers and RF/LO sideband, many frequency converters using carrier suppressed double sideband (CS-DSB) modulation are investigated [14], [15]. Nevertheless, the beating of $\pm$1st order sidebands will also bring about the mixing spurs. Hence, carrier suppressed single-sideband (CS-SSB) modulation is usually employed in frequency converters [16]. They present a reconfigurable microwave photonic converter by means of using two modulators and optical filters. But the parallel structure is quite complicated, and the requirement for consistency of modulators is extremely strict in the meanwhile. From then on, Fang et al. realized ultra-broadband microwave frequency down-conversion based on the optical frequency comb (OFC) to tackle these negative effects introduced by the two modulators [17]. Still, the structure of this system is complex and costly due to the OFC generator used in the scheme. Therefore, easier methods based on Brillouin frequency shifter can be applied in the microwave photonic frequency converter [18]–[20].

In this paper, a simple and flexible all-optical microwave photonic method for frequency converter is proposed and experimentally demonstrated to up/down-convert the signals of different frequency range. The key technologies of this scheme are the Brillouin selective amplification property and the Brillouin frequency shifter performance based on the stimulated Brillouin scattering (SBS) effect. The use of SBS is to generate the Stokes light and providing a gain for the system. The narrow gain spectrum generated by the SBS effect can generate the Stokes light whose frequency is down-shifted by v_b. The signal processed by the SBS effect is modulated by the MZM. After being filtered through the tunable optical bandpass filter (TBPF), the microwave signals at 1 to 15 GHz can be up-converted while the microwave signals at 11 to 29 GHz can be down-converted by means of tuning the TBPF. The proposed structure is simple and has tolerance to the dispersion introduced by optical fiber because the number of the laser is only one. In addition, the electronic bottleneck effect and limited bandwidth can be solved since the all-optical microwave photonic frequency converter is free of electrical components.

2. Operation Principle

Fig. 1 depicts the structure of the proposed all-optical microwave photonic frequency converter. A light wave at v_c emitted from a laser diode (LD) is split into two paths by a 3-dB optical coupler (C1). The light in the upper branch is amplified by an erbium-doped optical fiber amplifier (EDFA) and thereafter gets into port-1 of the optical circulator (OC) via an isolator (ISO), which is used to isolate the inverse transmission. The magnified signal is employed as the pump light for the SBS effect. The so-called Stokes wave at $v_c - v_b$ generated is regarded as the processed optical carrier in a length of 14-km single-mode fiber (SMF) which is used as Brillouin gain medium. The processed optical carrier from port-3 of the OC is modulated by the RF signal and filtered by the TBPF which determines to up/down-conversion. Subsequently, the treated signal is amplified by
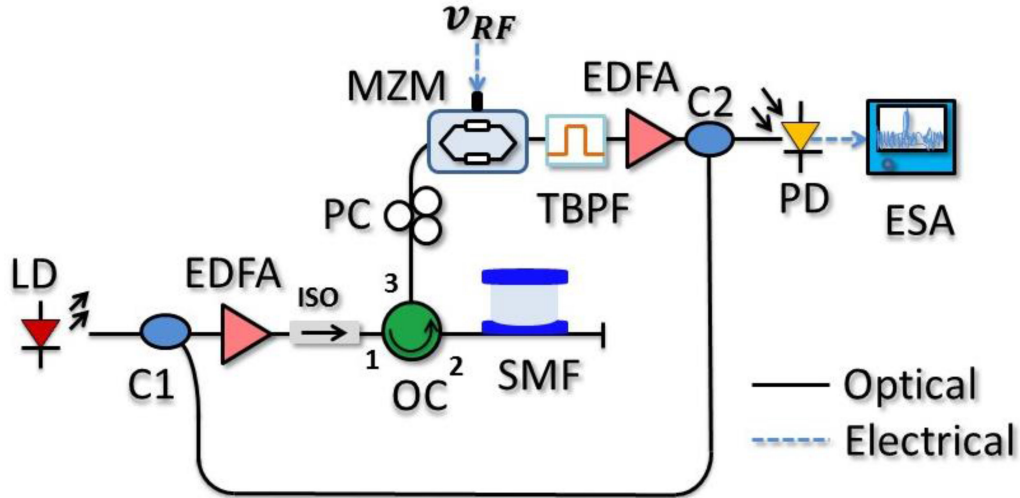
Fig. 1. Schematic diagram of the microwave photonic frequency converter. LD: laser diode, C: optical coupler, EDFA: erbium-doped optical fiber amplifier, ISO: optical isolator, OC: optical circulator, SMF: single mode fiber, PC: Polarization Controller; MZM: Mach-Zehnder modulator, TBPF: tunable optical passband filter, PD: photodetector, ESA: electrical spectrum analyzer. Solid line: optical path. Dotted line: electrical path.

the second EDFA and then coupled into another 3-dB optical coupler (C2) with the optical signal of the lower branch in the scheme, as shown in Fig. 1. After coupling, the dual-wavelength output is heterodyned at a high-speed photodetector (PD) to produce a signal after frequency converting.

The amplified continuous-wave at v_c via the first EDFA is considered as the pump wave to stimulate the SBS effect when the power of the pump light exceeds the threshold condition. The SBS process arises from electrostriction, in which a time-varying electric field creates a time-varying change in density of the material system (i.e., acoustic excitation). The acoustic wave modulates the refractive index of the medium, which induces both amplifying and absorbing resonances in the vicinity of the applied laser frequencies [21]. A periodic grating structure will be formed by the acoustic wave. The SBS effect refers to two beams of optical signals which are transmitted in opposite directions [22]. Once the power of the pump light exceeds the threshold condition of the pump light, the SBS effect will occur when the propagating Stokes wave with frequency of $v_c - v_b$ as the optical carrier can be generated from port-3 of the OC in the opposite direction, as illustrate in Fig. 2(a). After the SBS effect, the pump wave with the frequency of v_c will generate a Stokes wave at $v_c - v_b$, and the energy transfer will take place. The continuous wave at v_c is in decay because of transferring energy to reverse-transmitted Stokes wave at the same time.

The Brillouin gain spectrum $g(f)$ and loss spectrum $\alpha(f)$ of the SBS effect in the fiber can be expressed as [23]

$$g(f) = \frac{g_0}{2} \frac{\left(\Gamma_B/2\right)^2}{v^2 + \left(\Gamma_B/2\right)^2} + j\frac{g_0}{4} \frac{v\Gamma_B}{v^2 + \left(\Gamma_B/2\right)^2}, \tag{1}$$

$$\alpha(f) = -\frac{g_0}{2} \frac{\left(\Gamma_B/2\right)^2}{v^2 + \left(\Gamma_B/2\right)^2} - j\frac{g_0}{4} \frac{v\Gamma_B}{v^2 + \left(\Gamma_B/2\right)^2}. \tag{2}$$

Where $g_0 = g_B\, I_p L_{eff}/A_{eff}$, g_B and Γ_B are the line-center gain and Brillouin linewidth of the fiber respectively, v is the frequency offset from the center of Brillouin gain (for $g(f)$) or loss (for $\alpha(f)$), I_p
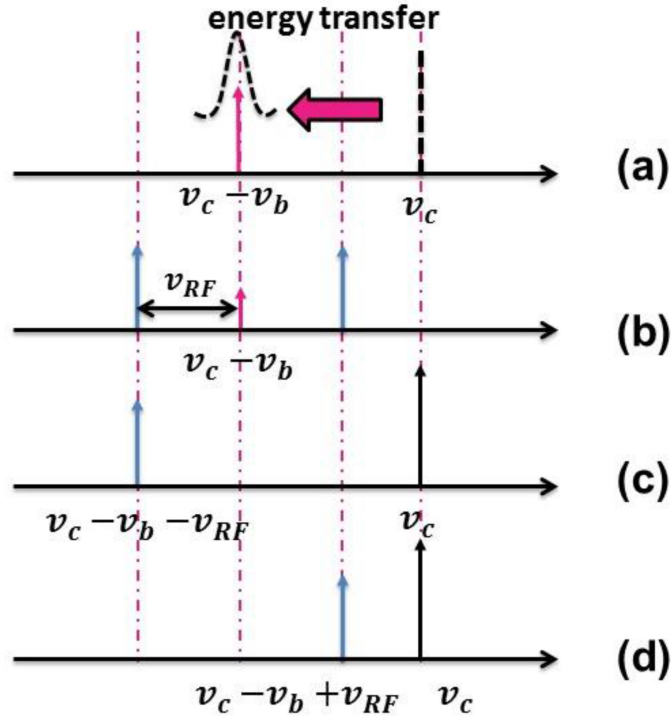
Fig. 2. Principle of operation. (a) The counter-propagated Stokes light produced by the energy transfer of the SBS process. (b) Output spectrum of the MZM. (c) Optical spectrum after the TBPF filters out the right sideband. (d) Optical spectrum when the right sideband is reserved.

is the power of the pump light, and L_{eff} and A_{eff} devote the effective fiber length and effective mode area of the SMF.

Afterwards, the Stokes wave is modulated by the RF signal at v_{RF} in the MZM, as shown in Fig. 2(b). The single drive MZM is set to operate at minimum transmission point (MITP) so that the carrier suppressed double sideband (CS-DSB) signal can be generated after the SBS effect. Under the small-signal modulation condition, the output optical field of the CS-DSB signal can be written after the expansion of Bessel function as follows [24]:

$$E_{MZM}(t) \propto \frac{\sqrt{2}}{2} E_0 J_1(\beta) \{\exp[j2\pi(v_c - v_b - v_{RF})t + \exp[j2\pi(v_c - v_b + v_{RF})t]\}, \qquad (3)$$

where $\beta = \pi V_m/2V_\pi$ is the modulation index of the MZM, E_0 is the amplitude of the processed optical carrier, v_{RF} is the RF signal to the modulator, V_m and V_π represent the amplitude of the modulated signal and the half-voltage of the MZM. $J_n(\beta)$ is the nth-order Bessel function of the first kind.

Then the CS-DSB signal passes through the TBPF to filter out one sideband and the suppressed single sideband (CS-SSB) signal is obtained. The TBPF filters out the right sideband the scheme is the so-called down-converter, while the up-converter is done under the condition of the right sideband is reserved, as illustrated in Fig. 2(c) and Fig. 2(d). As for up-converter and down-converter, the formulas can be described as

$$E_{TBPF\_up}(t) \propto \frac{\sqrt{2}}{2} E_0 J_1(\beta) \{\exp[j2\pi(v_c - v_b - v_{RF})t\}, \qquad (4)$$

$$E_{TBPF\_down}(t) \propto \frac{\sqrt{2}}{2} E_0 J_1(\beta) \{\exp[j2\pi(v_c - v_b + v_{RF})t\}. \qquad (5)$$
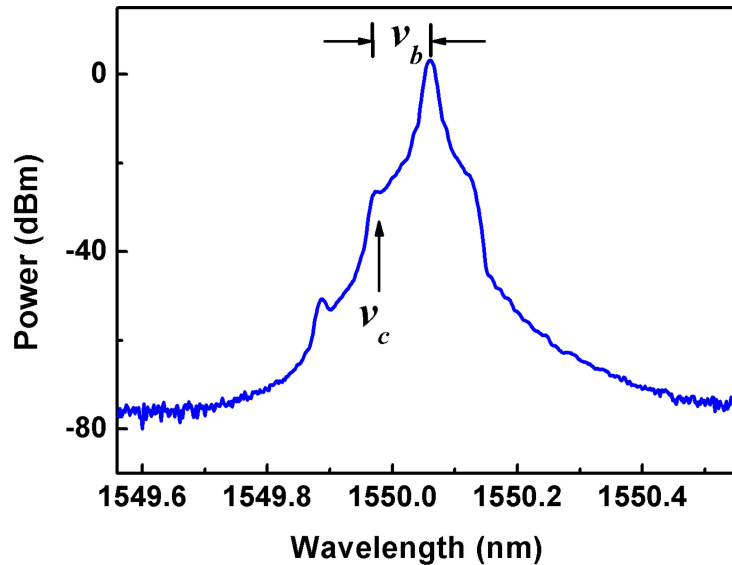
Fig. 3. Optical spectrum of counter-propagated Stokes light produced by the energy transfer in the SBS process. An SBS-based frequency shifter is incorporated to generate Stokes wave whose frequency is down-shifted by v_b.

The signals after the TBPF and the light wave from the LD are converted to the microwave signal by a high-speed PD after coupling. The current detected by PD of up-converter and down-converter can be described as

$$I_{up\_converter} \approx E_0^2 \, J_1 \, (\beta) \cos\left[(v_{RF} + v_b) \, t\right], \tag{6}$$

$$I_{down\_converter} \approx E_0^2 \, J_1 \, (\beta) \cos\left[(v_{RF} - v_b) \, t\right]. \tag{7}$$

Eventually, the frequency of the up/down-converted signal can be described as

$$v_1 = v_{RF} + v_{b,} \tag{8}$$

$$v_2 = v_{RF} - v_{b,} \tag{9}$$

where v_1 and v_2 are the frequencies of the output up-converted signal and the down-converted signal, respectively.

3. Experimental Results

A proof-of-concept experiment is carried out based on the schematic and shown in Fig. 1. A light wave with a wavelength of 1549.98 nm is launched into the SMF via the OC after enlarging by the first EDFA. When the power of the signal exceeds the threshold, the SBS effect will occur and Brillouin frequency shift v_b is about 10.82 GHz. Fig. 3 indicates the optical spectrum of the counter-propagated Stokes light produced by the SBS effect in the length of 14-km SMF through an optical spectrum analyzer (OSA, Yokogawa AQ6370D).

Then the Stokes light spreads into the MZM (Oclaro AM-20). The half-wave voltage V_π of the MZM is 5.5 V, and the MZM is driven by the RF signal from an analog signal generator (Keysight E8257D), which can provide the signal frequency from 1 to 15 GHz and 11 to 29 GHz with frequency intervals of 1 GHz to be converted. To attain the optimum optical carrier-to-sideband ratio of the modulated signal, the MZM is biased at minimum transmission point. Thus, the bias voltage of the MZM is about 5.2 V in the experiment. A TBPF (Yenista Optics XTM-50) is used as reserving the upper sideband or the lower sideband. The modulated signal is amplified to 11.8 dBm using the second EDFA. After the TBPF, an EDFA operated at constant current control (ACC) mode
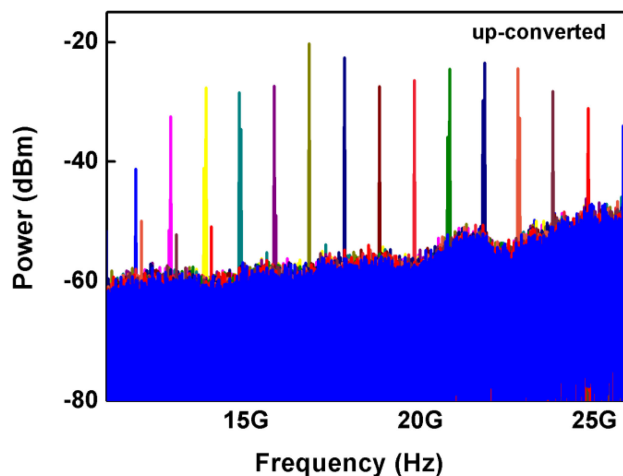
Fig. 4. Electrical spectrum of the output up-converted signal after measuring at PD. The frequency from 1 to 15 GHz with frequency intervals of 1 GHz can be up-converted to 11.82 to 25.81 GHz, and the frequency values of the abscissa are 11.82, 12.83, 13.84, 14.79, 15.80, 16.80, 17.81, 18.82, 19.82, 20.83, 21.84, 22.79, 23.80, 24.80, 25.81 GHz from left to right.
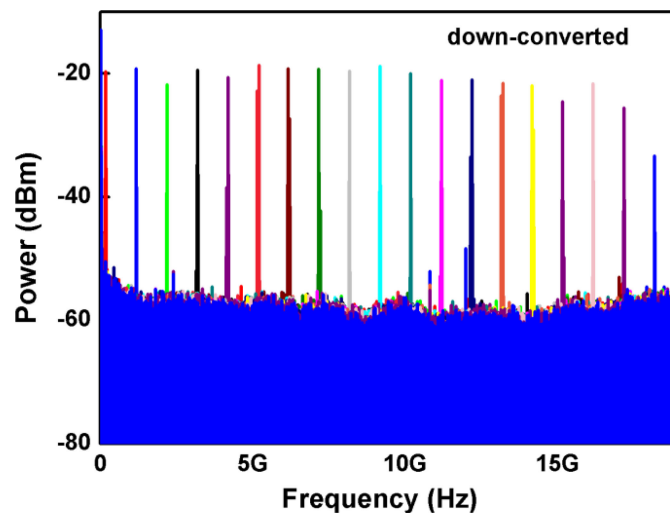

Fig. 5. Measured electrical spectrum of the output down-converted signal after the PD. The frequency-to-be-converted signal from 11 to 29 GHz with frequency intervals of 1 GHz can be down-converted from 0.17 to 18.18 GHz, and the frequency values of the abscissa are 0.17, 1.18, 2.18, 3.19, 4.20, 5.20, 6.16, 7.16, 8.17, 9.18, 10.18, 11.19, 12.20, 13.20, 14.16, 15.16, 16.17, 17.18, 18.18 GHz from left to right.

is applied to compensate the insertion loss of the TBPF and the MZM. Owing to the imbalance between the upper/lower sidebands and the light wave at 1549.98 nm, up/down-conversion is realized by beating optical carrier and sidebands. We measured the spectrum by an electrical spectrum analyzer (ESA, Keysight N9010A) which can observe the signal from 10 Hz to 26.5 GHz, the spectrum of the output of the PD is shown in Figs. 4 and 5. It can be seen that the frequency from 1 to 15 GHz with frequency intervals of 1 GHz will be up-converted to 11.82 to 25.81 GHz, as shown in Fig. 4. By the same token, the frequency-to-be-converted signal from 11 to 29 GHz with frequency intervals of 1 GHz can be down-converted from 0.17 to 18.18 GHz, as indicated in Fig. 5. Since the frequency bandwidth is dependent highly on the experimental devices including the MZM, the ESA and the PD. The frequency converter can achieve a wider bandwidth without
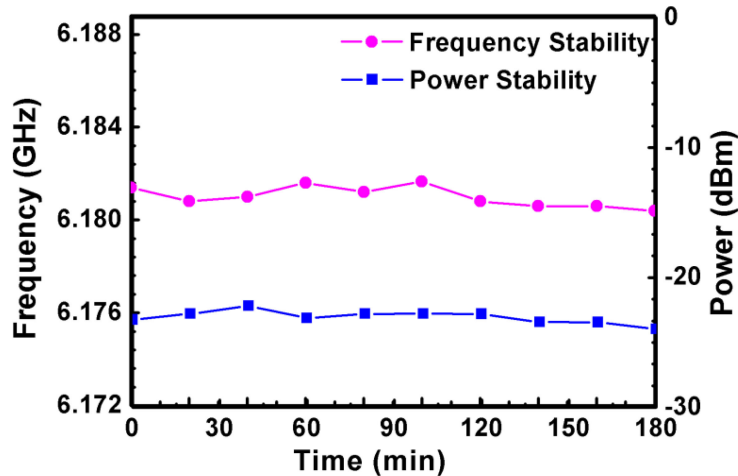
Fig. 6. Frequency and power stability of the generated down-converted signal when the input signal is 17 GHz, which is measured every 20 min in 3 hours.

being limited by the bandwidth of the devices. Because he system is sensitive to the polarization rotation, the reasons caused by polarization rotation could make the power fluctuation. However, using better performance devices or controlling polarization well can make the system more stable.

Besides, the Brillouin frequency shift can be expressed as [25]

$$v_b = 2nv_A/\lambda_p, \tag{10}$$

where n and v_A denote the effective refractive index of the optical fiber and the velocity of the acoustic, respectively, λ_p is the wavelength of the pump wave. The effective refractive index and wavelength of the pump wave will develop a fluctuation with the changes of environmental parameters such as vibration temperature. The Brillouin frequency shift will drift with temperature, strain, etc. Measurements of the electrical spectrum are carried out every 20 min in 3 hours for the sake of studying the frequency stability of the proposed photonic frequency down-converter when the input signal is 17 GHz, as depicted in Fig. 6. It is found that the frequencies fluctuate in the range of 0.0013 from 6.1804 GHz to 6.1817 GHz in 3 hours, and the maximum deviation from the average value of 6.1811 GHz is 0.0105%. On the other hand, the RF power is also measured in the experiment, and the recorded average peak power is −23.07 dBm. As time goes on, the fluctuations in power are significant because the SBS effect in the fiber is sensitive to parameters, and these fluctuations are caused by temperature changes of the environment and the devices [26]. To solve this problem, the system can be stabilized by placing it in a temperature-controlled room.

4. Summary and Conclusions

In summary, we have demonstrated and experimentally proposed the principle of a novel and flexible all-optical microwave frequency photonic converter with ultra-wideband based on SBS and TBPF. A SBS-based frequency shifter is adopted to generate the Stokes wave as the optical carrier whose frequency is at $v_c − v_b$. Hence, the LO source is not required in the frequency converter. After being modulated by the MZM, the modulated signal is processed by the TBPF. The TBPF filters out the right sideband the scheme is the so-called down-converter, while the scheme is an up-converter under the condition of the right sideband is left. Consequently, it has a wide bandwidth operation of 1 to 15 GHz for up-conversion and 11 to 29 GHz for down-conversion. The system is simple, in the meanwhile, the all-optical microwave photonic frequency converter is free of the electrical components. Consequently, the proposed structure may have the potential to be utilized in the signal processing in the radio-over-fiber systems as the scheme is simple and convenient.

References

[1] R. Y. Miyamoto and T. Itoh, "Retrodirective arrays for wireless communications," *IEEE Microw. Mag.*, vol. 3, no. 1, pp. 71–79, Mar. 2002.

[2] C. S. Brès, S. Zlatanovic, A. O. Wiberg, and S. Radic, "Reconfigurable parametric channelized receiver for instantaneous spectral analysis," *Opt. Express*, vol. 19, no. 4, pp. 3531–3541, 2011.

[3] A. Agarwal, T. Banwell, and T. K. Woodward. "Optically filtered microwave photonic links for RF signal processing applications," *J. Lightw. Technol.*, vol. 29, no. 16, pp. 2394–2401, Aug. 2011.

[4] E. H. Chan and R. A. Minasian. "High conversion efficiency microwave photonic mixer based on stimulated Brillouin scattering carrier suppression technique," *Opt. Lett.*, vol. 38, no. 24, pp. 5292–5295, 2013.

[5] D. S. Shin *et al.*, "Optoelectronic RF signal mixing using an electroabsorption waveguide as an integrated photodetector/mixer," *IEEE Photon. Technol. Lett.*, vol. 12, no. 2, pp. 193–195, Feb. 2000.

[6] Y. Wang *et al.*, "Ultra-wideband microwave photonic frequency downconverter based on carrier-suppressed single-sideband modulation," *Opt. Commun.*, vol. 410, pp. 799–804, 2018.

[7] Z. Tang and S. Pan, "A reconfigurable photonic microwave mixer using a 90° optical hybrid," *IEEE Trans. Microw. Theory Tech.*, vol. 64, no. 9, pp. 3017–3025, Sep. 2016.

[8] R. Schnabel *et al.*, "Polarization insensitive frequency conversion of a 10-channel OFDM signal using four-wave-mixing in a semiconductor laser amplifier," *IEEE Photon. Technol. Lett.*, vol. 6, no. 1, pp. 56–58, Jan. 1994.

[9] G. Maury, A. Hilt, T. Berceli, B. Cabon, and A. Vilcot, "Microwave-frequency conversion methods by optical interferometer and photodiode," *IEEE Trans. Microw. Theory Tech.*, vol. 45, no. 8, pp. 1481–1485, Aug. 1997.

[10] C. Bohemond, T. Rampone, and A. Sharaiha, "Performances of a photonic microwave mixer based on cross-gain modulation in a semiconductor optical amplifier," *J. Lightw. Technol.*, vol. 29, no. 16, pp. 2402–2409, Aug. 2011.

[11] S. Fu, W.-D. Zhong, P. Shum, Y. J. Wen, and M. Tang, "Simultaneous multichannel photonic up-conversion based on nonlinear polarization rotation of an SOA for radio-over-fiber systems," *IEEE Photon. Technol. Lett.*, vol. 21, no. 9, pp. 563–565, May 2009.

[12] G. K. Gopalakrishnan, W. K. Burns, and C. H. Bulmer, "Microwave-optical mixing in LiNbO/sub 3/modulators," *IEEE Trans. Microw. Theory Tech.*, vol. 41, no. 12, pp. 2383–2391, Dec. 1993.

[13] T. Li, E. H. W. Chan, X. Wang, X. Feng, B. O. Guan, and J. Yao, "Broadband photonic microwave signal processor with frequency up/down conversion and phase shifting capability," *IEEE Photon. J.*, vol. 10, no. 1, Feb. 2018, Art. no. 5500112.

[14] E. H. Chan and R. A. Minasian, "Microwave photonic downconverter with high conversion efficiency," *J. Lightw. Technol.*, vol. 30, no. 23, pp. 3580–3585, Dec. 2012.

[15] T. Jiang, S. Yu, Q. Xie, J. Li, and W. Gu, "Photonic downconversion based on optical carrier bidirectional reusing in a phase modulator," *Opt. Lett.*, vol. 39, no. 17, pp. 4990–4993, 2014.

[16] Y. Wang *et al.*, "All-optical microwave photonic downconverter with tunable phase shift," *IEEE Photon. J.*, vol. 9, no. 6, Dec. 2017, Art. no. 5503408.

[17] X. Fang, M. Bai, X. Ye, J. Miao, and Z. Zheng, "Ultra-broadband microwave frequency down-conversion based on optical frequency comb," *Opt. Express*, vol. 23, no. 13, pp. 17111–17119, 2015.

[18] Y. G. Shee *et al.*, "All-optical generation of a 21 GHz microwave carrier by incorporating a double-Brillouin frequency shifter," *Opt. Lett.*, vol. 35, no. 9, pp. 1461–1463, 2010.

[19] T. Shimizu, K. Nakajima, K. Shiraki, K. Ieda, and I. Sankawa, "Evaluation methods and requirements for the stimulated Brillouin scattering threshold in a single-mode fiber," *Opt. Fiber Technol.*, vol. 14, no. 1, pp. 10–15, 2008.

[20] R. A. Minasian, E. H. W. Chan, and X. Yi, "Microwave photonic signal processing," *Opt. Express*, vol. 21, no. 19, pp. 22918–22936, 2013.

[21] Z. Zhu, D. J. Gauthier, and R. W. Boyd, "Stored light in an optical fiber via stimulated Brillouin scattering," *Science*, vol. 318, no. 5857, pp. 1748–1750, 2007.

[22] Y. Wang *et al.*, "Wideband tunable up-converting optoelectronic oscillator based on gain–loss compensation technology and stimulated Brillouin scattering," *Opt. Quantum. Electron.*, vol. 51, no. 2, 2019, Art no. 43.

[23] D. Wang *et al.*, "Wide-range, high-accuracy multiple microwave frequency measurement by frequency-to-phase-slope mapping," *Opt. Laser Technol.*, vol. 123, 2020, Art. no. 105895.

[24] W. Zhai, A. Wen, and D. Shan, "Photonic generation and transmission of frequency-doubled triangular and square waveforms based on two Mach–Zehnder modulators and a sagnac loop," *J. Lightw. Technol.*, vol. 37, no. 9, pp. 1937–1945, May 2019.

[25] H. Peng *et al.*, "Tunable DC-60 GHz RF generation utilizing a dual-loop optoelectronic oscillator based on stimulated Brillouin scattering," *J. Lightw. Technol.*, vol. 33, no. 13, pp. 2707–2715, Jul. 2015.

[26] X. Bao, Q. Yu, and L. Chen, "Simultaneous strain and temperature measurements with polarization-maintaining fibers and their error analysis by use of a distributed Brillouin loss system," *Opt. Lett.*, vol. 29, vol. 12, pp. 1342–1344, 2004.